# Silicon Based 1 × $M$ Wavelength Selective Switch Using Arrayed Waveguide Gratings With Fold-Back Waveguides

Fumi Nakamura, Hideaki Asakura, Keijiro Suzuki, Ken Tanizawa, Minoru Ohtsuka, Nobuyuki Yokoyama, Kazuyuki Matsumaro, Miyoshi Seki, Kazuhiro Ikeda, Shu Namiki, Hitoshi Kawashima, and Hiroyuki Tsuda

***Abstract*—The design of a novel 1 × $M$ fold-back type wavelength selective switch (WSS), which has fewer waveguide crossings than a conventional integrated WSS, is reported. The WSS is composed of interleavers, 1 × $M$ optical switches, and arrayed waveguide gratings (AWGs). Switches are combined with AWGs by fold-back waveguides, and each AWG works as both a demultiplexer and multiplexer thus avoiding center wavelength mismatch caused by fabrication errors. Waveguide crossings cause excess crosstalk and loss in lightwave circuits. By using a fold-back architecture the number of crossings can be reduced to less than half that of a conventional design. We discuss the operating principle, the design method, and the scalability of the fold-back type WSS. Furthermore, the switching operation of a 200-GHz spacing, 20-channel, 1 × 2 silicon WSS in a fold-back configuration on a 5 mm × 10 mm SOI chip is demonstrated. This has 15 waveguide crossings in a path, of which six are additional crossings with monitor waveguides. The average insertion loss and average extinction ratio are 29.6 dB and 10.9 dB, respectively.**

***Index Terms*—Arrayed waveguide grating, optical networking, waveguide crossing, wavelength division multiplexing, wavelength selective switch.**

## I. Introduction

A 1 × $M$ wavelength selective switch (WSS) is an optical element with which optical signals of specific wavelengths can be switched from an input port into any number of $M$ output ports. A WSS is typically composed of wavelength demultiplexers, switching elements, and multiplexers. The demultiplexer decomposes the inserted wavelength division multiplexed (WDM) signal into separate signals depending on wavelength. Each signal is routed to a switching element which sends the signal to one of a number of output ports. The signals are then multiplexed at each output port. By using multiple output WSSs, signals can be added to and dropped from any of the directions depending on the wavelength. WSSs enable the introduction of colorless, directionless, and contentionless reconfigurable optical add/drop multiplexers (CDC-ROADM) at network nodes in WDM optical communication systems [1], [2].

Several types of WSS with multiple output ports have been demonstrated, such as free-space optics based-WSSs [3]–[5], waveguide-based integrated WSSs [6]–[12], and hybrid type WSSs, which combine planar lightwave circuits (PLC) with liquid crystals on silicon (LCOS) or microelectromechanical systems (MEMS) mirror switches [13]–[15]. Free space optics based WSSs with LCOS switches have been put into practical use since a large port count and low insertion loss can be achieved. However, this requires the assembly of several lenses and switches with high accuracy; therefore, they are very costly, and the device size is large. By comparison with those devices, WSSs integrated into lightwave circuits are suitable for mass production with CMOS process technology, and are potentially low cost. In particular, silicon waveguide-based WSSs can be integrated with high density because waveguides on silicon have a vast refractive index difference between the silicon core and the silica cladding.

The conventional waveguide type 1 × $M$ WSS, which employs arrayed waveguide gratings (AWGs) as demultiplexers, $N_{\mathrm{ch}}$ 1 × $M$ Mach-Zehnder interferometer (MZI) switches for selecting the output ports, and $M$ AWGs for multiplexing, has $N_{\mathrm{ch}}$ wavelength channels into which signals are arbitrarily directed, as shown in Fig. 1 [6]. The WSS with this configuration has ($M$-1) ($N_{\mathrm{ch}}$-1) waveguide crossings in a path, causing excess loss and crosstalk. Thus, the number of crossings depends on the numbers of ports and channels, and the scalability of conventional type WSSs is limited. We proposed and demonstrated several designs of WSS, such as a wavefront control configuration without crossings [9] and a fold-back configuration [10]–[12], of which

Manuscript received September 26, 2020; revised November 27, 2020; accepted December 26, 2020. Date of publication December 31, 2020; date of current version April 16, 2021. This work was supported in part by JSPS KAKENHI Grant JP18H01501 and Grant JP19J21526 and in part by Support Center for Advanced Telecommunications Technology Research, Foundation. *(Corresponding author: Fumi Nakamura.)*

Fumi Nakamura, Hideaki Asakura, and Hitoshi Kawashima are with the Faculty of Science and Technology, Department of Electronic and Electrical Engineering, Keio University, Kanagawa 223-8522, Japan (e-mail: f_nakamura@tsud.elec.keio.ac.jp; askr@tsud.elec.keio.ac.jp; kawashima-h@aist.go.jp).

Keijiro Suzuki, Minoru Ohtsuka, Nobuyuki Yokoyama, Kazuyuki Matsumaro, Miyoshi Seki, Kazuhiro Ikeda, Shu Namiki, and Hiroyuki Tsuda are with the National Institute of Advanced Industrial Science and Technology (AIST), Ibaraki 305-8569, Japan (e-mail: k.suzuki@aist.go.jp; ohtsuka.minoru@aist.go.jp; nobuyuki-yokoyama@aist.go.jp; k-matsumaro@aist.go.jp; seki.miyoshi@aist.go.jp; kaz.ikeda@aist.go.jp; shu.namiki@aist.go.jp; tsuda@elec.keio.ac.jp).

Ken Tanizawa is with the National Institute of Advanced Industrial Science and Technology (AIST),Quantum ICT Research Institute, Tamagawa University, Tokyo 194-8610, Japan (e-mail: tanizawa@lab.tamagawa.ac.jp).

Color versions of one or more of the figures in this article are available online at https://doi.org/10.1109/JLT.2020.3048585.

Digital Object Identifier 10.1109/JLT.2020.3048585

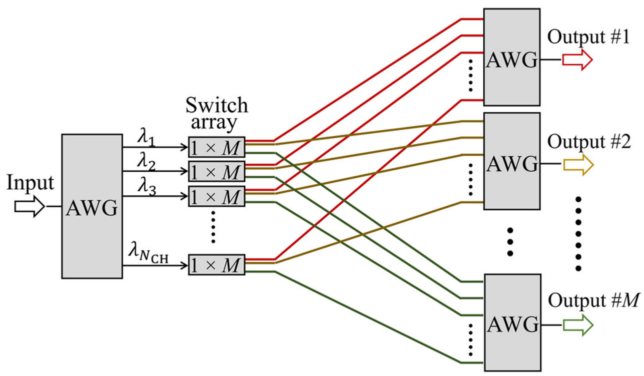


Fig. 1. Schematic of conventional $1 \times M$ WSS with $N$ch wavelength channels, composed of an AWG for the input, $1 \times M$ switches, and $M$ AWGs for the outputs. The WSS has ($M$-1) ($N$ch-1) waveguide crossings in a path.

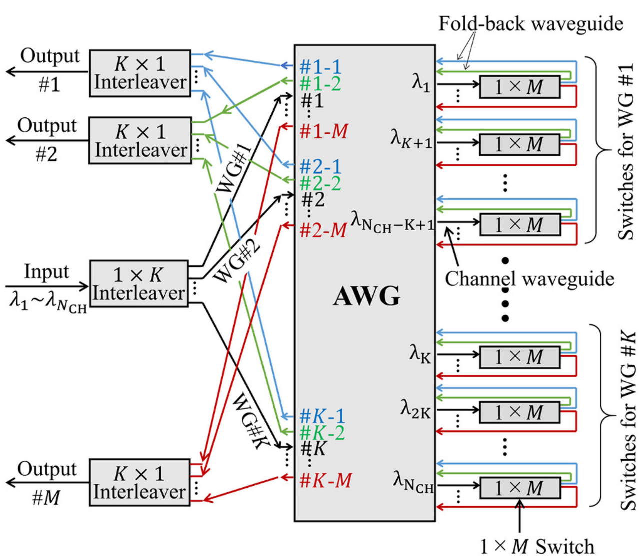


Fig. 2. Schematic of $1 \times M$ fold-back type WSS, which is made up of one $1 \times K$ interleaver for the input, $K \times 1$ interleavers for the outputs, an AWG and $1 \times M$ optical switches. Fold-back waveguides are used to link the outputs of the switches with the AWG.

power consumption is lower than the other configuration to solve this problem.

In this paper, we present our analysis of a silicon WSS with a fold-back architecture. The proposed WSS employs interleavers for demultiplexing and multiplexing as well as an AWG. In Section II, the operating principle and the method used to design the WSS are presented. We also use numerical simulation to examine its scalability. In Section III, the characteristics of a $1 \times 2$ fold-back type, 20-channel, 200-GHz spacing WSS are demonstrated. Finally, we conclude this study in Section IV.

## II. Configuration of a $1 \times M$ Fold-Back Type WSS

### A. *Configuration of a Fold-Back Type WSS With a Single AWG*

A schematic of a $1 \times M$ fold-back type WSS is shown in Fig. 2, which consists of one $1 \times K$ interleaver, a single AWG, $N_{ch}$ $1 \times M$ optical switches, and $M$ $K \times 1$ interleavers. The AWG is employed as both a demultiplexer and a multiplexer which avoids center wavelength mismatch caused by fabrication errors. The outputs from the $1 \times M$ switches are input to the AWG via the fold-back waveguides.

The $1 \times K$ interleaver at the input port splits the WDM signal into $K$ wavelength groups, which are delivered to corresponding positions of the AWG where they are divided into $N_{ch}$ wavelength signals. Each separate signal is inserted from a channel waveguide into a $1 \times M$ switch and, after selecting an arbitrary output port, reinserted into the AWG via a fold-back waveguide for multiplexing. Eventually, the wavelength signals come out from the selected output port as a WDM signal after being combined by the $K \times 1$ interleaver.

In this design, the maximum number of waveguide crossings in a path is expressed as 3/2 $M$ ($K$-1) where $K$ is the number of wavelength groups and $M$ the number of output ports. The number of crossings in the fold-back configuration depends only on the number of output ports $M$, not on the number of wavelength channels $N_{ch}$, since the number of wavelength groups $K$ is determined by the number of output ports $M$. The conventional monolithic $1 \times M$ WSS consisting of an AWG and $N_{ch}$ $1 \times M$ switches has ($M$-1) ($N_{ch}$-1) crossings in a path; therefore, the advantage of the fold-back type WSS is obvious when a large number of wavelength channels is included. For example, to design a $1 \times 4$ WSS for the C band with 100 GHz channel spacing, of which the number of channel $N_{ch}$ is 40, the number of waveguide crossings is 42 in the fold-back configuration with a single AWG, when $K$ is 2$M$. This is less than half the number of crossings of the conventional design, which is 117.

### B. *Design Method of 1 × M Fold-Back Type AWG*

In the fold-back type WSS, the AWG used for demultiplexing is also utilized for multiplexing signals from the fold-back waveguides in the reverse direction. In this section we describe the way in which the AWG is designed. Fig. 3 shows (i) a schematic of an AWG attached to optical switches in a $1 \times M$ fold-back type WSS and (ii) a detailed schematic of the 2nd slab waveguide in the AWG. As shown in Fig. 3(i), the two edges of the first slab waveguide are marked as the $x_1$-axis and $x_2$-axis, and the edges of the second slab waveguide are marked as the $x_3$-axis and the $x_4$-axis, respectively. The origins of these axes are at the centers of each edge. The wavelength groups #1, #2, …#$K$, which come from the $1 \times K$ interleaver, are input into the first slab waveguide from the waveguides positioned at $x_{\text{in}1}$, $x_{\text{in}2}, \ldots x_{\text{in}\,K}$ along the $x_1$-axis. After propagating through the first slab waveguide, the arrayed waveguides, and the second slab waveguide, the wavelength group #$j$, which contains $\lambda_j$, $\lambda_{(K+j)}, \ldots \lambda_{(N\text{-}1)\,K+j}$ is demultiplexed, and the individual signals are coupled to the channel waveguides, which are located at $x_4 = x_{\text{out }j1}, x_{\text{out }j2}, x_{\text{out }jN}$, distributed around the position $x_4 = x_{\text{out}j}$ as detailed in Fig. 3(ii). Here, $N$ is the number of channels in each wavelength group, which is expressed as $N = N_{ch}\,/\,K$.

The path length difference between adjacent array waveguides, $\Delta l$, is given by (1), in which the center wavelength is $\lambda_0$,

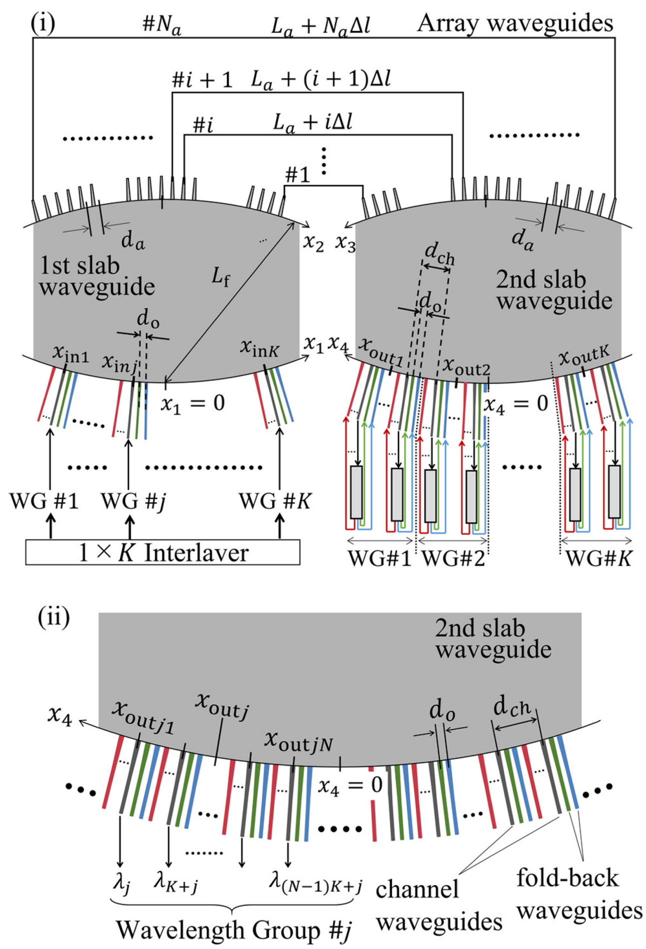


Fig. 3. (i) Schematic of Arrayed waveguide grating with 1 × *M* switches in a 1 × *M* fold-back WSS. (ii) Detailed schematic of the edge of the 2nd slab waveguide.

and the effective refractive index of the array waveguide at the center wavelength is $n_{\mathrm{a}}$ [18].

$$\Delta l = \frac{m\lambda_0}{n_{\mathrm{a}}} \tag{1}$$

The integer *m* is the diffraction order, given by,

$$m = \frac{cn_{\mathrm{a}}}{\nu_{\mathrm{FSR}} n_{\mathrm{g}} \lambda_0} \tag{2}$$

In (2), $\nu_{\mathrm{FSR}}$ is the free spectral range of the AWG and $n_{\mathrm{g}}$ is the group index given by (3), where $n_{\mathrm{a}}$ is the effective index of the array waveguides.

$$n_{\mathrm{g}} = n_{\mathrm{a}} - \lambda \frac{dn_{\mathrm{a}}}{d\lambda} \tag{3}$$

When an AWG is utilized for demultiplexing only one WDM signal, $\nu_{\mathrm{FSR}}$ should satisfy the condition $\nu_{\mathrm{FSR}} \geq N_{\mathrm{ch}}\Delta\nu$, where $\Delta\nu$ is the frequency spacing of the WSS. In the case of a fold-back WSS, the fold-back type AWG needs to decompose multiple wavelength groups from different positions on the $x_1$-axis and $\nu_{\mathrm{FSR}}$ needs to satisfy the following condition.

$$\nu_{\mathrm{FSR}} \geq N_{\mathrm{ch}}\Delta\nu_{\mathrm{AWG}} = N_{\mathrm{ch}} K \Delta\nu \tag{4}$$

The parameter, $\Delta\nu_{\mathrm{AWG}}$, is the frequency spacing between signals coupled to adjacent channel waveguides, and it is the frequency spacing between adjacent channels of the wavelength group $K\Delta\nu$.

The radii of curvature of the first and second slab waveguides are equal to $L_{\mathrm{f}}$, which is given by,

$$L_{\mathrm{f}} = \frac{n_{\mathrm{s}} d_{\mathrm{a}} d_{\mathrm{ch}} \nu_{\mathrm{FSR}}}{\lambda_0 \Delta\nu_{\mathrm{AWG}}} \tag{5}$$

where $n_{\mathrm{s}}$ is the effective refractive index of the slab waveguides, $d_{\mathrm{a}}$ is the arrayed waveguide spacing along the $x_2$-axis and $x_3$-axis, and $d_{\mathrm{ch}}$ is the channel waveguide spacing at the outer edge of the second slab waveguide, i.e., the $x_4$-axis. We assume that the waveguides along the $x_4$-axis, both the channel waveguides and the fold-back waveguides, are arranged at equal intervals $d_{\mathrm{o}}$, so the spacing $d_{\mathrm{ch}}$ should be $(M+1)d_{\mathrm{o}}$, and the slab length $L_{\mathrm{f}}$ is proportional to the number of output ports *M* and the number of wavelength channels $N_{\mathrm{ch}}$.

The position of the central channel waveguide for the wavelength group #*j*, $x_{\mathrm{out}\ j}$, is given by (6).

$$x_{\mathrm{out}j} = N d_{\mathrm{ch}} \left( \frac{K}{2} - j \right) \tag{6}$$

If the location of the input waveguide for the wavelength group #*j* on the $x_1$-axis, $x_{\mathrm{in}j}$ is arranged symmetrically with respect to the position of the central channel waveguide $x_{\mathrm{out}j}$ on the $x_4$-axis, that is $x_{inj} = -x_{\mathrm{out}j}$, the signal inserted at $x_1 = x_{\mathrm{in}j}$ is dispersed so that the center wavelength $\lambda_0$ is focused at $x_{\mathrm{out}\ j}$. Therefore it is necessary to adjust the input position $x_{\mathrm{in}j}$ according to the central wavelength of the wavelength group #*j*, $\lambda_{0j}$, as given by the following equation.

$$x_{\mathrm{in}j} = -x_{\mathrm{out}j} + \frac{d_{\mathrm{ch}}}{\Delta\nu_{\mathrm{AWG}}} \left( \frac{c}{\lambda_0} - \frac{c}{\lambda_{0j}} \right) \tag{7}$$

Each wavelength channel comes back into the AWG from one of *M* fold-back waveguides, which is shifted by $\Delta x$ from the $x_4$ position of the corresponding channel waveguides, such as $x_{\mathrm{out}j1}, x_{\mathrm{out}j2}, \ldots x_{\mathrm{out}jN}$, and coupled into the output waveguide at $x_1 = x_{\mathrm{in}j} - \Delta x$ as wavelength group #*j* after propagating through the second slab waveguide, the array waveguides, and the first slab waveguide.

## C. Fold-Back Type WSS Using Multiple AWGs

When the fold-back type AWG is shared for all of the wavelength groups as described in Section II.B, its diffraction order *m* is restricted by the following condition, according to (2) and (4).

$$m \leq \frac{cn_{\mathrm{a}}}{N_{\mathrm{ch}}\Delta\nu_{\mathrm{AWG}} n_{\mathrm{g}} \lambda_0} \tag{8}$$

Hence it is difficult to demultiplex signals with a single AWG when the WSS needs a large number of wavelength channels and wavelength groups because the diffraction order should be an integer. In this case, the WSS could use multiple AWGs. Fig. 4 shows the configuration of a 1 × *M* fold-back type WSS using *K* AWGs, as an example of AWG division. The number of waveguide crossings is (*K*-1) (*M*-1).

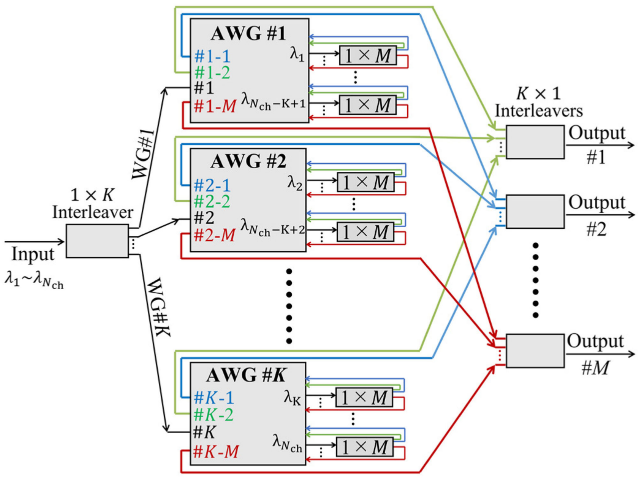


Fig. 4. Schematic showing the configuration of a $1 \times M$ fold-back type WSS, which consists of one $1 \times K$ interleaver, $K \times 1$ interleavers for the outputs, K AWGs and $1 \times M$ optical switches. The outputs of the switches and the AWGs are linked together with fold-back waveguides.

The condition for the FSR of the AWG is given in (9), where the number of AWGs is $N_{\mathrm{AWG}}$.

$$\nu_{\mathrm{FSR}} \geq \frac{N_{\mathrm{ch}}}{N_{\mathrm{AWG}}} \Delta\nu_{\mathrm{AWG}} = \frac{N_{\mathrm{ch}}}{N_{\mathrm{AWG}}} K \Delta\nu \quad (9)$$

The larger the number of AWGs the WSS is composed of, the smaller FSR each AWG has. However, each AWG has a different center wavelength shift due to fabrication errors, and it needs individual center wavelength adjustment to the wavelength grid of interleavers. In the proposed WSS, the number of AWGs should be optimized by considering the center wavelength mismatch, the FSR, and the number of waveguide crossings.

## D. Scalability of Fold-Back Type WSS

According to sections B and C, the number of wavelength groups $K$ is a significant parameter, since the number of intersections is smaller with smaller $K$. Nevertheless, as the frequency spacing of the channels coupled to the adjacent waveguides of the AWG, $\Delta\nu_{\mathrm{AWG}} = (K/N_{\mathrm{AWG}})\Delta\nu$, becomes smaller, the wavelength spread becomes wider with respect to the channel waveguide spacing $d_{\mathrm{ch}} = (M+1)d_{\mathrm{o}}$, so the passband becomes narrower with smaller $K$.

Fig. 5 shows the calculated transmittance of a 100-GHz spacing, 40-channel, $1 \times 2$ fold-back type WSS, in which the number of wavelength groups $K$ is (i) 2 and (ii) 8, and in which each pair of adjacent channels are allocated to Output#1, #2. The WSSs were designed using the equations in II.B, where the center wavelength $\lambda_0$ is 1.55 µm, the array waveguide spacing $d_{\mathrm{a}}$ is 2.0 µm, and the fold-back waveguide spacing $d_{\mathrm{o}}$ is 2.0 µm. The effective refractive index of the slab waveguide $n_{\mathrm{s}}$ and the arrayed waveguide $n_{\mathrm{a}}$ were calculated with Finite Element Method (FEM) mode solver and approximated to a linear expression of free space wavelength $\lambda_0$ within the range of C-band for taking wavelength dispersion into account. The index of slab waveguide $n_{\mathrm{s}}$ = - 0.56133 $\lambda_0$ + 3.71488 and that of arrayed waveguide $n_{\mathrm{a}}$ = - 0.70934 $\lambda_0$ + 3.84272 are used in the calculations, where the unit of wavelength $\lambda_0$ is. $\mu$m. Each $1 \times 2$ Mach-Zehnder interferometer is assumed to consist of a $1 \times 2$ multimode interferometer (MMI) coupler, two arms, and a $2 \times 2$ MMI coupler. Propagation in the slab waveguides was analyzed as a one-dimensional Fourier transform [19] using the fast Fourier transform (FFT) method [20] in MATLAB. In the simulation, the loss due to crossings was not considered, and the calculated results include losses due to higher-order light after propagation in the slab waveguide and coupling losses to the arrayed waveguide.

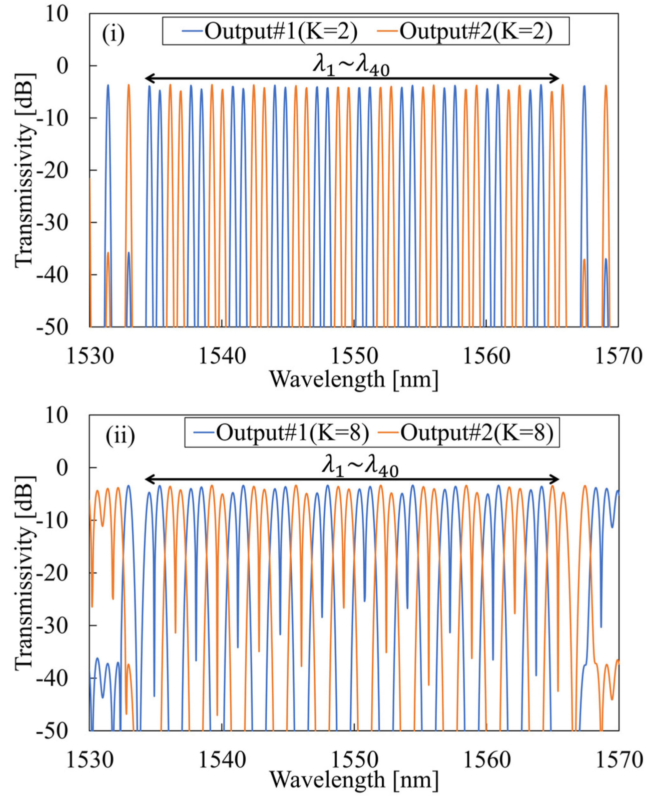


Fig. 5. Calculated transmittance of 100-GHz spacing, 40-channel, $1 \times 2$ fold-back type WSS using a single AWG when each pair of adjacent channels are allocated to Output#1, 2, of which the number of wavelength groups (i) K = 2, (ii) K = 8.

Table I shows the characteristics of a 100-GHz spacing, 40-channel, $1 \times 2$ fold-back type WSS with the wavelength groups $K$ = 2, 4, 8. All the WSSs use a single AWG. The design of the WSSs with $K$ = 2 and 8 are the same as those shown in Fig. 5. By comparing Fig. 5(i) and 5(ii), the passband of the WSS in which the number of wavelength groups $K$ is 2, is narrower than that when $K$ is 8. However, the large number of wavelength groups not only increases the waveguide crossings, but also the crosstalk. According to Table I, when the number of wavelength groups $K$ is twice of the number of output ports $M$, such as $K$ = 4 in the $1 \times 2$ WSS, the wider passband can be achieved without the occurrence of considerable crosstalk.

TABLE I
CALCULATED CHARACTERISTICS OF 100-GHZ SPACING, 40-CHANNEL, 1 × 2 WSS WITH VARIOUS NUMBER OF WAVELENGTH GROUPS $K$

| Parameter | $K = 2$ | $K = 4$ | $K = 8$ |
|---|---|---|---|
| Maximum Number of waveguide crossings in a path | 3 | 9 | 21 |
| Diffraction order of AWG | 9 | 4 | 2 |
| 3dB-passband [GHz] | 16.3 | 31.4 | 48.9 |
| Crosstalk in the 50 GHz band [dB] | 58.3 | 52.0 | 29.9 |
| Maximum insertion loss at channel wavelength [dB] | 4.8 | 4.8 | 5.0 |

The diffraction order of the AWG $m$ for each value of $K$ is designed so that the maximum insertion loss at the channel wavelength is around 5 dB. Thus, with the fold-back configuration the loss difference between channel wavelengths can be reduced by designing a smaller diffraction order at the cost of device size.

Evaluation of the scalability of 1 × $M$ fold-back type WSSs with 100 GHz spacing, 40 channels with various numbers of AWGs is shown in Table II. Here, the extinction ratio is the transmittance difference between the ON and OFF states at the same output. The diffraction order for each WSS was determined to reduce the maximum loss to around 5 dB, and in each case, the number of wavelength groups $K$ is twice the number of output ports $M$. The maximum insertion loss and minimum extinction ratio are shown in Table II; both of the case without considering phase error and with considering phase error. In order to taking phase error into account, the standard deviation on the arrayed waveguide width $\sigma_w$ was assumed to 0.83 nm [17] and the corresponding refractive index deviation was added to $n_a$ at each arrayed waveguide. Due to fabrication width deviation, the extinction ratio is degraded to 13.0 dB at the minimum and the maximum insertion loss is increased to about 13 dB. The extinction ratio of fold-back WSS using smaller number of AWGs is less affected by fabrication error since its AWGs have smaller diffraction order and shorter arrayed waveguides.

The table also includes evaluations of crossing numbers for a conventional 1 × $M$ WSS comprising 1 × $M$ switches and AWGs, which is obtained from ($M$-1) ($N_{ch}$-1). The conventional 1 × 2, 1 × 4, and 1 × 8 WSS with 40 channels has 39, 117, and 273 crossings in an optical path at most, and this could result in 1.092 dB, 3276 dB, and 7.644 dB loss, respectively, even if the low loss intersection design reported in reference [16] is employed, where the insertion loss per intersection is 0.028 ± 0.009 dB at 1550 nm. The number of crossings can be reduced to less than that of a conventional design by adopting a fold-back design. In the case of a 1 × 8 fold-back type WSS with 4 AWGs, there are 120 waveguide crossings, and the insertion loss due to the intersections is estimated to be 3.36 ± 1.080 dB. In the 45-nm node CMOS process on 300 mm wafer, the size of a single shot of lithography is 33 mm × 26 mm. As shown in Table II, the 1 × 8 WSS that we design can fit the shot size.

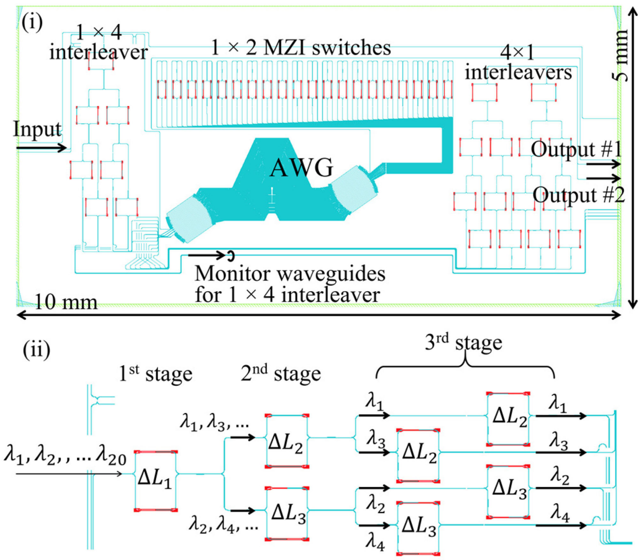


Fig. 6. (i) 200 GHz spaced 20 channel 1 × 2 fold-back type WSS which includes a 1 × 4 interleaver, twenty 1 × 2 MZI switches, and two 4 × 1 interleavers. The chip size is 5 mm × 10 mm. (ii) Enlarged view of 1 × 4 interleaver for the input, which is composed of three stages of asymmetric mach-zehnder interferometers. The 3rd stage is employed to increase the extinction ratio.

## III. MONOLITHIC 1 × 2 FOLD-BACK TYPE WSS

To demonstrate the feasibility of the fold-back configuration, we designed and fabricated a 1 × 2 fold-back type WSS in silicon photonics. The channel spacing $\Delta\nu$ is 200 GHz, and the number of channels $N_{ch}$ is 20 [11], [12].

### A. Device Design

The mask layout of the WSS is shown in Fig. 6. The chip size is 5 mm × 10 mm. The number of output ports $M$ is 2, and the number of wavelength groups $K$ is 4. The 1 × 2 WSS consists of a 1 × 4 interleaver for the input, one AWG combined with twenty 1 × 2 MZI switches by fold-back waveguides, and two 4 × 1 interleavers for the output ports. The interleavers for combining have the same design as the interleaver for separating and are used in the opposite direction. The important AWG design parameters are given in Table III.

The number of unavoidable waveguide crossings is assumed to be 9 when there are 4 wavelength groups, according to Section II. In this 1 × 2 WSS, the maximum number of waveguide crossings in one path is 15, because AWG monitor waveguides and input interleaver monitors cause 6 additional waveguide crossings. The number of intersections is being improved in this 1 × 2 fold-back WSS by comparison with a conventional 20 channel, 1 × 2 WSS which would have 19 crossings. More improvement would be obtained in terms of the number of crossings with a WSS with more channels.

The interleaver is composed of three-stages of asymmetric Mach-Zehnder interferometers. The first stage interferometer,

TABLE II
CHARACTERISTICS OF 100-GHz SPACING, 40-CHANNEL, WSS WITH VARIOUS NUMBER OF OUTPUT PORTS AND NUMBER OF AWGs

| | 1 × 2 WSS | | 1 × 4 WSS | | 1 × 8 WSS | |
|---|---|---|---|---|---|---|
| Number of waveguide crossings in the conventional design | 39 | | 117 | | 273 | |
| Number of AWGs | 1 | 4 | 2 | 8 | 4 | 16 |
| Number of waveguide crossings | 9 | 3 | 30 | 21 | 120 | 105 |
| Diffraction order of AWGs | 4 | 22 | 4 | 22 | 3 | 18 |
| Chip size on silicon photonics | 15 mm × 7 mm | 15 mm × 5 mm | 20 mm × 15 mm | 20 mm × 13 mm | 30 mm × 25 mm | 30 mm × 25 mm |
| Maximum insertion loss at channel wavelength[dB] ( with phase error ) | 4.8 (13.2) | 4.9 (13.4) | 4.8 (10.6) | 4.9 (11.9) | 4.6 (9.5) | 4.9 (11.0) |
| Minimum extinction ratio at channel wavelength [dB] ( with phase error ) | 53.4 (28.5) | 53.2 (15.1) | 69.0 (23.4) | 68.5 (13.0) | 68.3 (21.5) | 68.2 (14.0) |
| Estimated loss due to crossings by using low loss intersection[16] [dB] | 0.252 | 0.084 | 0.840 | 0.588 | 3.360 | 2.940 |

TABLE III
DESIGN VALUES OF AWG IN FABRICATED 200 GHz SPACED 20 CHANNEL 1 × 2 FOLD-BACK WSS

| Parameter | Symbol | Value |
|---|---|---|
| Center wavelength [μm] | $\lambda_0$ | 1.55 |
| Number of AWGs | $N_{AWG}$ | 1 |
| Free spectral range of AWG [THz] | $\nu_{FSR}$ | 23.1 |
| Frequency spacing of AWG [GHz] | $\Delta\nu_{AWG}$ | 800 |
| Number of array waveguides | $N_a$ | 270 |
| Diffraction order | $m$ | 6 |
| Length difference between neighboring array waveguides [μm] | $\Delta l$ | 3.385 |
| Radius of curvature of slab waveguides [μm] | $L_f$ | 636.708 |

of which the FSR is 400 GHz, separates the input signal into two wavelength groups, and the second stage, of which the FSR is 800 GHz, divides the two-wavelength groups into four wavelength groups. The third stage is adopted to increase the extinction ratio. The arm length differences of the interferometers, $\Delta L_1$, $\Delta L_2$, and $\Delta L_3$ are 195.202 μm, 97.460 μm, and 97.601 μm, respectively.

## B. Measured Characteristics

The 1 $\times$ 2 fold-back WSS chip was fabricated on a 300 mm SOI wafer at a 45-nm node CMOS pilot line featuring immersion ArF lithography. TiN phase shifters are employed on the interleavers to compensate for the phase error, and heaters on the MZI switches are used for selecting the output port.

Fig. 7 shows the experimental results for a 1 $\times$ 2 fold-back type WSS when odd and even channels were switched to Output #1 and Output #2. Fig. 7(i) and 7(ii) show the transmittance of Output #1 and Output #2, respectively.

The average insertion loss without chip coupling loss is 30.4 dB and 28.9 dB at Output #1 and Output #2 and the extinction ratio is 13.1 dB and 9.8 dB at Output #1 and Output #2, respectively. The total current applied to the heaters on the input and output interleavers to compensate for the phase error was 116 mA and the average current applied to the MZI switches to select Output #1 and Output #2 were 7.8 mA and 7.0 mA respectively.

## C. Discussion

The experimental switching operation of fold-back configuration has been successfully demonstrated with fabricated 1 $\times$ 2 WSS with single AWG. However, the performances such as the insertion loss and the extinction ratio were worse than the calculated results in Section II. D.

The loss breakdown of 1 $\times$ 2 fold-back type WSS is shown in Table IV. The loss of each component was measured by using the test circuit, which was fabricated on the same wafer of the WSS. The interleaver and 1 $\times$ 2 MZI switch had insertion losses of 2.89 dB and 3.86 dB, respectively. The insertion loss of AWG was 3.12 dB for demultiplexing and 3.49 dB for multiplexing. The average transmission loss of one waveguide crossing was 0.35 dB within the range of C-band. The total loss was 21.5 dB. The experimental average insertion loss of the integrated WSS was 29.6 dB. The additional loss, which is estimated to 8.1 dB, may be attributed to the poorly compensated phase errors at the 4 $\times$ 1 interleavers in the output side and the mismatch of the selected wavelengths. The interleaver is composed of three

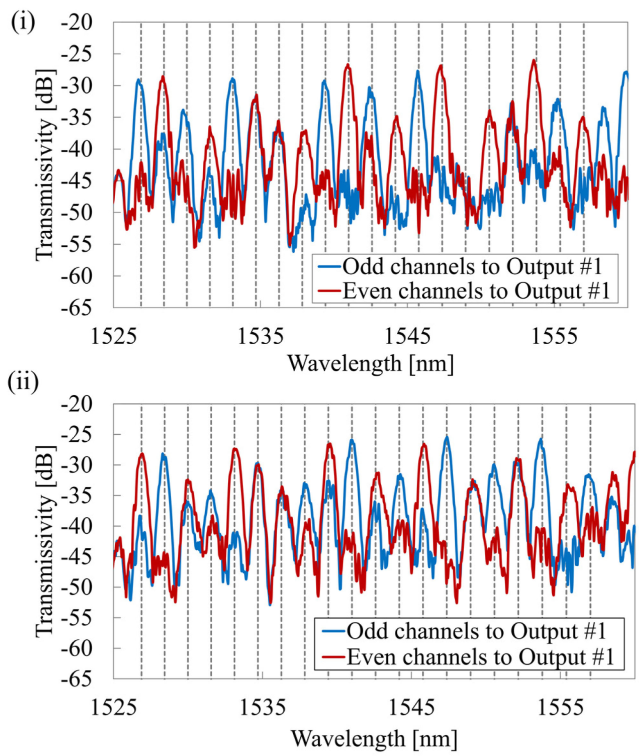


Fig. 7. Transmittance of (i) Output #1 and (ii) Output #2, in the cases that the even channels and odd channels are switched to Output #1. Channel #6, 7, 15, and 17 didn't work since current could not be applied to the TiN phase shifters on the corresponding MZI switches due to broken wires.

TABLE IV
LOSS BREAKDOWN OF 200 GHZ SPACED 20 CHANNEL
1 × 2 FOLD-BACK WSS

| Components | Loss (test circuit) | Loss (optimized) |
|---|---|---|
| 1 × 4 interleaver for input | 2.89 dB | 0.39 dB |
| AWG (demultiplexer) | 3.12 dB | 3.28 dB |
| 1 × 2 MZI switch | 3.86 dB | 0.13 dB |
| AWG (multiplexer) | 3.49 dB | 3.28 dB |
| 4 × 1 interleaver for output | 2.89 dB | 0.39 dB |
| 15 waveguide crossings | 5.25 dB | 0.36 dB |
| Total | 21.50 dB | 7.83 dB |

stages of asymmetric Mach Zehnder interferometers and its operated wavelength is affected by phase error at arm waveguides. The phase error at input 1 × 4 interleaver was compensated successfully by using monitor waveguides. However, output 4 × 1 interleavers didn't have monitors and the compensations of them are considered to be insufficient. This additional loss can be reduced by adding monitor waveguides in output side.

The achievable transmission loss of 1 × 2 WSS is also shown in Table IV. The insertion loss of each component can be improved sufficiently by optimizing its design and fabrication process. The reported 32 × 32 silicon optical matrix switch which fabricated in the same CMOS plot line of AIST, achieved 6.4 dB on-chip loss, even the lightwave propagated 32 MZI switches and 31 waveguide intersections [21]. The loss of 1 × 4 interleaver with three-stage configuration is estimated to 0.39 dB. The loss of the optimized MZI swich and the crossing structure is 0.13 dB and 0.024 dB, respectively. The average insertion loss of AWG simulated with phase error was 3.28 dB. The total loss of 1 × 2 fold-back WSS can be reduced from 29.6 dB to 7.83 dB with such improvements.

The extinction ratio was mainly determined by two factors: the extinction ratio of the AWG and 4 × 1 interleaver in the output side. 1 × 4 interleaver for input can be tuned using monitor ports and has less effect on the extinction ratio. In the test circuit fabricated simultaneously with the WSS, the average extinction ratio of AWG was 19.1 dB at channel wavelengths. The experimental average extinction ratio of the WSS is 10.9 dB and it is smaller than the test AWG. The additional degradation of the extinction was also caused by the poor adjustment of output 4 × 1 interleavers due to lack of monitor ports. The output interleaver works as a filter and multiplexers. Therefore, the mismatch of the center wavelengths lowers the extinction ratio effectively. By introducing monitor waveguides to the 4 × 1 output interleaver, the average extinction ratio of about 19 dB, which is limited by the extinction ratio of AWG, could be obtained.

By using fine process nodes and introducing phase error trimming, the extinction ratio can be improved. Practically, the addition of the cleanup filters after AWG may be acceptable solution with current silicon photonics technology.

The multiple path interference (MPI) is common problem of silicon photonics devices. In particular, the edge coupling without anti-reflection coating on both facets was used for our experiment, and it leads to ripples in transmission characteristics. The low-loss, matched coupling between a fiber and a spot-size converter will relax this problem. For the internal reflections at the slab-array boundary and at the MMI coupler may have some effect on the characteristics. These structures should be carefully designed to reduce the reflection.

## IV. CONCLUSION

We have reported on the operating principle, the design method, and the scalability of a fold-back type WSS, which has a smaller number of waveguide intersections, which cause extra losses and crosstalk in lightwave circuits. According to our estimate of the scalability, a 1 × 8 fold-back type WSS with 4 AWGs can be monolithically integrated on a 30 mm × 25 mm chip with only 120 intersections between the silicon waveguides. The switching operation was demonstrated with a 200-GHz spacing, 20-channel, 1 × 2 fold-back type silicon WSS. The maximum number of crossing was 15 in a path, where 9 were internal crossings in the fold-back configuration with 4 wavelength groups and 6 come from crossings with monitor waveguides. The average insertion loss was 29.6 dB, and the average extinction ratio was 10.9 dB.

## References


[1] S. Gringeri *et al.*, "Flexible architectures for optical transport nodes and networks," *IEEE Commun. Mag.*, vol. 48, no. 7, pp. 40–50, Jul. 2010.

[2] D. M. Marom *et al.*, "Survey of photonic switching architectures and technologies in support of spatially and spectrally flexible optical networking [invited]," *J. Opt. Commun. Netw.*, vol. 9, no. 1, pp. 1–26, Jan. 2017.

[3] D. M. Marom *et al.*, "Wavelength-Selective $1 \times k$ switches using free-space optics and MEMS micromirrors: Theory, design, and implementation," *J. Lightw. Technol.*, vol. 23, no. 4, pp. 1620–1630, Apr. 2005.

[4] Y. Ishii *et al.*, "MEMS-based $1 \times 43$ wavelength-selective switch with flat passband," presented at the 35th Eur. Conf. Opt. Commun., Vienna, Austria, 2009, pp. 1–2.

[5] M. Iwama *et al.*, "Low loss $1 \times 93$ wavelength selective switch using PLC-based spot size converter," presented at the Eur. Conf. Opt. Commun., Valencia, Spain, 2015, pp. 1–3.

[6] C. R. Doerr *et al.*, "Monolithic flexible-grid $1 \times 2$ wavelength-selective switch in silicon photonics," *J. Lightw. Technol.*, vol. 30, no. 4, pp. 473–478, Feb. 2012.

[7] T. Yoshida *et al.*, "Switching characteristics of a 100-GHz-spacing integrated 40-$\lambda$ $1 \times 4$ wavelength selective switch," *IEEE Photon. Technol. Lett.*, vol. 26, no. 5, pp. 451–453, Mar. 2014.

[8] Y. Ikuma *et al.*, "Low-loss integrated $1 \times 2$ gridless wavelength selective switch with a small number of waveguide crossings," presented at the Eur. Conf. Exhib. Opt. Commun., Amsterdam, Netherlands, 2012, pp. 1–3.

[9] F. Nakamura *et al.*, "Integrated silicon photonic wavelength-selective switch using wavefront control waveguides," *Opt. Express*, vol. 26, no. 10, pp. 13573–13589, May 2018.

[10] F. Nakamura *et al.*, "Silicon photonics based $1 \times 2$ wavelength selective switch using fold-back arrayed-waveguide gratings," *IEICE Electron. Express*, vol. 15, no. 14, pp. 20180532–20180532, Jul. 2018.

[11] H. Asakura, K. Sugiyama, and H. Tsuda, "Design of a $1 \times 2$ wavelength selective switch using an arrayed-waveguide grating with fold-back paths on a silicon platform," presented at the 21st Optoelectron. Commun. Conf., Niigata, Japan, 2016, pp. 1–3.

[12] F. Nakamura *et al.*, "Characteristics of $1 \times 2$ silicon wavelength selective switch using arrayed-waveguide gratings with fold-back waveguides," presented at the 18th Int. Conf. Opt. Commun. Netw., Huangshan, China, 2019, pp. 1–2.

[13] D. M. Marom *et al.*, "Hybrid free-space and planar lightwave circuit wavelength-selective $1 \times 3$ switch with integrated drop-side demultiplexer," presented at the 31st Eur. Conf. Opt. Commun. (ECOC 2005), Glasgow, U.K., vol. 4, 2005, pp. 993–994.

[14] K. Sorimoto *et al.*, "Compact and phase-error-robust multilayered AWG-based wavelength selective switch driven by a single LCOS," *Opt. Express*, vol. 21, no. 14, pp. 17131–17149, Jul. 2013.

[15] K. Suzuki *et al.*, "Ultra-High port count wavelength selective switch employing waveguide-based I/O frontend," presented at the Opt. Fiber Commun. Conf., Los Angeles, USA, 2015, pp. 1–3.

[16] Y. Ma *et al.*, "Ultralow loss single layer submicron silicon waveguide crossing for SOI optical interconnect," *Opt. Express*, vol. 21, no. 24, pp. 29374–29382, Dec. 2013.

[17] T. Horikawa *et al.*, "The impacts of fabrication error in si wire-waveguides on spectral variation of coupled resonator optical waveguides," *Microelectron. Eng.*, vol. 156, pp. 46–49, Apr. 2016.

[18] K. Okamoto, "Arrayed-waveguide grating," in *Fundamentals of Optical Waveguides*, 2nd ed., ch. 9, sec. 3. Amsterdam, Netherlands: Elsevier, 2006, pp. 423–428.

[19] P. Munoz, D. Pastor, and J. Capmany, "Modeling and design of arrayed waveguide gratings," *J. Lightw. Technol.*, vol. 20, no. 4, pp. 661–674, Apr. 2002.

[20] D. H. Bailey and P. N. Swarztrauber, "A fast method for the numerical evaluation of continuous fourier and laplace transforms," *SIAM J. Sci. Comput.*, vol. 15, no. 5, pp. 1105–1110, Sep. 1994.

[21] K. Suzuki *et al.*, "Low insertion loss and power efficient $32 \times 32$ silicon photonics switch with extremely-high-$\Delta$ PLC connector," presented at the Opt. Fiber Commun. Conf., San Diego, USA, 2018, pp. 1–3.